Journal of Materials Chemistry A

Accepted Manuscript

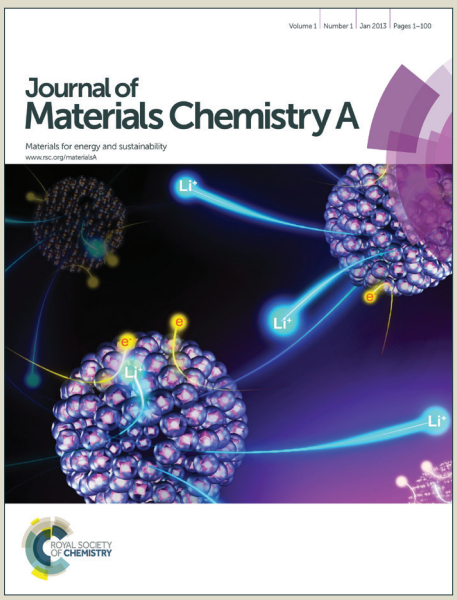

ROYAL SOCIETY OF CHEMISTRY

www.rsc.org/materialsA

Self-Protected Nickel-Graphene Hybrid Low Density 3D Scaffolds

Moab Rajan Philip[a], Tharangattu N. Narayanan[b,*], M. Praveen Kumar[b], Shashi Bhushan Arya[a] and Deepak K. Pattanayak[b,*]

[a]National Institute of Technology, Surathkal, Karnataka, India.

[b]CSIR-Central Electrochemical Research Institute, Karaikudi, Tamilnadu, India.

(Corresponding Authors: tn_narayanan@yahoo.com (T. N. N.), pattanayak1977@gmail.com (D. K. P.))

ABSTRACT

Development of low density metallic foams is highly intriguing for various applications. Moreover, synthesis of hierarchical 3-dimensional structures of graphene is also receiving tremendous attention in recent days due to their unique electrical, thermal, mechanical and chemical properties. Here, we demonstrate a novel method for the bulk production of graphene protected, freestanding, low density (0.03-0.15 g/cc) metallic nickel (Ni) foam (NiG) by a simple polyol assisted chemical route. This hybrid NiG foam is synthesized in air, and during its synthesis, Ni is protected by graphene from its oxidation. These magnetic scaffolds can be used for various energy and environmental applications, and also can be structurally reinforced with other polymers. Poly methyl methacrylate (PMMA) is infiltrated into the Ni / NiG foams and the subsequent annealing of Ni / PMMA composite foam in Ar-H_2 atmosphere at 900^{o}C leads to the formation of large area graphene by the graphitisation of PMMA on Ni. This large area graphene is separated and studied for its properties.

KEYWORDS

Metallic Foams, 3D Graphene, Polyol Process, Mechanical Reinforcement, Hybrid Foams.

Introduction

Various functional and structural derivatives of graphene were developed during the last few years after understanding their importance in energy and environment related fields.[1-4] These include 2-dimensional (2D) forms of graphene such as graphene oxide (GO),[5-7] graphene nanoribbons,[8-12] various doped graphene,[13-15] and 3D forms of graphene such as graphene/GO aerogels,[16-18] their hydrogels,[19-22] ultra-low density sponges[23-26] and graphene based various composites.[27,28] Among these various forms, 3D graphene foams / sponges caught the attention of researchers due to their applications in various fields, and the amenability in controlling porosity and density of the sponges to a large extent.[29,30] Various physical and chemical routes were realised in the recent past for the synthesis of micro / meso / macroscopic pores containing graphene / reduced graphene oxide (RGO) / GO sponges. High quality graphene sponges can be synthesized using template assisted chemical vapour deposition method, but it is time consuming and its yield is limited.[31-35] Bulk synthesis of graphene sponges mostly relies on chemical routes, and these routes mostly end up with RGO foams having deteriorated physical properties. Moreover, many of these freestanding RGO / GO foams need metal supports for applications and light weight and high surface area metal backbone is highly demanding (for example: supercapacitor applications).[36-39] Other disadvantages of such freestanding 3D graphene macrostructures are their poor electrical conductivity; either due to the low quality of graphene or high inter sheet resistance between the graphene layers or resistance due to the non-conducting covalent cross-linking agents, and low mechanical integrity.[40]

Flexible and porous metallic membranes or scaffolds are highly useful in various fields including in the fabrication of stretchable and wearable gadgets and flexible energy devices.[41] But low cost production of metallic scaffolds in bulk is rather challenging. Formation of oxide layer is yet another challenge in the development of highly reactive oxide

free metallic foams. Out of various metals, nickel (Ni) is a highly demanding metal useful for various electrochemical and catalytic applications.[42] Hence various attempts were made in the past for the development of porous Ni foams.[43] Metallic nickel foams are being fabricated commercially through various techniques like leaching and de-alloying. But they are relatively high density macro porous foams. Development of oxide free, magnetic, low density Ni foams is still remaining as a challenge. Commercial Ni foams have been used as templates for CVD based graphene growth, and later the Ni foams were dissolved using polymethyl methacrylate based transfer process.

Synthesis of Ni-graphene hybrid light weight foams in a single shot process will be of interesting for many applications. Other than the graphene synthesized over commercial porous Ni, recently Ni foams supported graphene sheets were developed through a multi-step process of electrophoretic deposition followed by chemical bath deposition.[44] Very recently, Huang et al. reported the direct formation of RGO and 3D lightweight Ni network composite foam by hydrohalic acid treatment and its further application in supercapacitors.[36] They also used commercial Ni foam for the development of the hybrid composite. Synthesis of light weight Ni nanoparticles using polyol process is reported in literature.[45] But, here we use a modified polyol process to develop large quantities of light weight NiG hybrid foams by employing nickel nitrate hexahydrate, ethylene glycol and RGO as starting materials. These developed hybrid foams were characterised and demonstrated for their application in various fields.

2. Experimental

2.1 Synthesis of graphene oxide and reduced graphene oxide

Graphene oxide (GO) was synthesized by an "improved method"[5] using graphite powder (Sigma Aldrich) as starting material. Graphite powder (2 g) was added to a mixture of conc.H_2SO_4 (98%, 360 mL, Sigma Aldrich) and phosphoric acid (40 mL, Sigma Aldrich)

where the volume ratio of sulphuric acid to phosphoric acid is kept at ratio 9:1.The complete mixing of the graphite in the solution was ensured by means of magnetic stirring, which was carried out at room temperature. After 10 minutes of stirring, $KMnO_4$ powder (14 g) (s d FINE–CHEM Ltd., India) was added gradually to the solution. The resultant mixed solution temperature was raised to 90^{o}C with continuous stirring for 24 hours. Then the solution was cooled down to room temperature and then placed in an ice bath. Subsequently, 14 mL of H_2O_2 (Sigma Aldrich) was added to the mixed solution and stirring was continued for 3 hours while keeping the beaker in an ice cooled bath. The reaction mixture was then washed with dilute HCl (5%, Sigma Aldrich) for several times to remove the excess metal ions. Reaction mixture was washed with deionised water and ethanol during the upcoming stages. Washing with deionised water was continued until the pH of the solution reaches neutral and a yellowish brown GO colloidal solution was obtained. This yellowish brown GO residue was collected after the centrifugation process and it was subsequently allowed to filter through a 0.24 μm filter paper with the help of a vacuum pump. The GO residue upon filtration was then collected and the sample was vacuum dried at 45^{o}C for 24 hours. The vacuum dried GO film was crushed and ground into fine GO powder using an agate mortar and pestle.

The yellow GO powder synthesized was converted to reduced graphene oxide (RGO) by hydrothermal process using hydrazine hydrate. Here, 0.2 g of GO powder was treated with a mixture of 93 mL of deionised water and 7 mL of hydrazine hydrate (Sigma Aldrich). The mixture was sonicated for 2 hours. The colloidal solution mixture was transferred to an autoclave. The autoclave was heated to a temperature of 180^{o}C for overnight. Upon finishing the reaction, the RGO residue was collected and washed with deionised water until the neutral pH is attained. The black coloured RGO residue collected over the filter paper was then subjected to vacuum drying at 45^{o}C for overnight. The residue was then crushed into fine powder using an agate mortar and pestle.

2.2 Fabrication of NiG foam

Nickel nitrate hexahydrate (35 g, Sigma Aldrich) and ethylene glycol (18 mL, Sigma Aldrich) were taken in a 100 mL beaker and the RGO powder (0.083 g) was added into the beaker and sonicated for 1 hour (the amounts of reactants mentioned here are the optimised values). The resultant mixture was then poured into a cylindrical glass dish which was pre-heated to a temperature of 250^{o}C. A sudden introduction of reactant solution in to the hot glass dish leads to the evolution of NO_2 gas and subsequent production of fluffy Ni foam incorporated with graphene. The same synthesis route is followed for the fabrication of Ni foams without addition of RGO powder.

2.3 Fabrication of PMMA reinforced composite foam

Aforementioned Ni / NiG foam is reinforced with PMMA using the following procedure: PMMA was dissolved in acetone and the mixture was sonicated for 15 minutes. This solution was drop casted on to the surface of shaped Ni / NiG foam. This PMMA impregnated Ni foam was allowed to dry in air at elevated temperatures (~ 50^{o}C). After the evaporation of acetone, porous Ni / PMMA / NiG / PMMA foam was obtained.

2.4 Fabrication of large area graphene using composite foam

Ni / PMMA foam was subjected to annealing under Ar-H_2 atmosphere at 900^{o}C. The heating rate was kept at 5^{o}C per minute and 900^{o}C temperature was maintained for 1 hour. After 1 hour, the furnace was cooled down to room temperature and the sample was removed from the furnace.

The fabricated Ni and NiG foams were characterised using various characterisation tools. The X-ray diffraction (XRD) study was carried out using Bruker X-ray powder diffractometer with Cu-K_α radiation (λ=0.154 nm) in the 2θ range 10-100 degree. The FTIR

spectra were recorded using Bruker Optic Gmbh, Tensor 27 Model in the range of 400 to 4000 cm^{-1}. The laser Raman spectra for the samples were collected using Renishaw U. K, Invia Raman microscope. The source employed was He-Ne laser having an excitation wavelength of 633 nm and having energy of 18 mW. The Raman spectra were collected using a back scattering geometry within an acquisition time of 40 seconds. The morphology of the foam was examined using a field-emission scanning electron microscope (Carl Zesis, SUPRA 55VPFEI, Germany) instrument. TEM analysis and selected area electron diffraction (SAED) patterns were recorded with a Technai model TEM instrument (FEI TECNAI $G^2$20) with an accelerating voltage of 200 kV. X-ray photoelectron spectroscopy (XPS) was carried out with PHI 5000 VersaProbe ULVAC instrument.

3. Results and discussion

Figure 1 represents the schematic fabrication process of magnetic Ni and NiG foams by polyol process. This process leads to the formation of ultralow density, magnetic Ni / NiG foams as depicted in figure 1. Sol-gel auto combustion is happening in the formation of porous metallic sponges. Ethylene glycol acts like a solvent and reducing agent and its boiling results in to the formation of a gel, and this gel subsequently expands and undergoes a violent exothermic reaction. The resulting material is a highly porous sponge. Incorporation of RGO in to the sol results in to a self-assembly process, resulting in to a graphene shell-Ni core hybrid material. The fluffy magnetic NiG foam formed inside the cylindrical dish surface was separated with the help of a permanent magnet. Inset FE-SEM image provided in Fig. 1 depicts an idea about the 3-dimensional (3D) interconnected morphology of the freestanding porous (meso and macro porous) NiG foams.

Figure 2 shows the detailed FE-SEM and TEM images of Ni and NiG foams. From the FE-SEM images shown in Fig. 2 (a) and (b), it is evident that the fabricated Ni and NiG foams are highly porous in microstructure. Open pores of diameter ranging from 3.5 nm –

200 μm were observed within the structure. The presence of a weak reducing agent like ethylene glycol (when compared to powerful reducing agents like sodium borohydride, lithium aluminium hydride) ensures that the generation and growth of the nuclei are moderately controlled, thereby resulting in the formation of agglomerated Ni foam instead of Ni nanoparticles.

Figures 2 (c) and (d) represent the EDS analysis of the samples conducted at different locations, across the cross sectional profile of NiG foam. The chemical composition of NiG foam conducted using an EDS revealed the presence of carbon and Ni. Figures 2 (e) and (f) represent the TEM images of Ni and NiG foams while their inset images correspond to SAED patterns. TEM images revealed the presence of interconnected Ni wrapped with graphene sheets in the NiG foam (Fig. 2f). SAED pattern of Ni foam showed the presence of nanocrystalline Ni particles, while the SAED of NiG showed the presence of Ni and graphene.

Figures 3 (a)-(c) show the XRD, FTIR and Raman spectra of NiG, Ni and graphene (RGO) samples respectively. XRD pattern recorded for Ni foam as observed in Fig. 3(a) revealed that the foam has considerable NiO presence, most probably forming as a sacrificial protective coating of NiO on the Ni surface. The identified sharp peaks at $2\theta = 37.25^0$, 43.27^0, 62.87^0, 75.41^0, 79.41^0, 95.06^0 are assigned to (111), (200), (220), (311), (222), (400) planes of cubic NiO (JCPDS No: 897130 with a=4.194 nm). The strong diffraction peaks for Ni were observed at $2\theta = 44.87^0$, 52.2^0, 76.6^0, 93.16^0 belong to (111), (200), (220) and (311) planes (JCPDS No: 870712) implying the presence of face centred cubic (FCC) Ni.

On the other hand, in the case of XRD of NiG foam, there is no signature of NiO formation in the sample. Hence it indicates that either graphene is completely protecting Ni from its oxidation during the synthesis or the amount is less than 2%, the detectable level of

XRD. The diffraction peak at 2θ = 23.9^{0}correspond to (002) plane hexagonal graphitic carbon.[3]

Figure 3 (b) shows FTIR spectra for graphene, NiG and Ni foams. Graphene and NiG foam show number of oxygen functionalities and this may be due to the residual functional groups in graphene (RGO).[46] Moreover, there is a considerable redshift (particularly to the major vibrations of C=C bond and –OH bond) in the FTIR peaks of NiG in comparison to that of graphene. This is due to the presence of metallic Ni over graphene. Moreover, the C=C stretching vibration (sp^2 hybridized) observed at 1580 cm^{-1} indicates the presence of graphene in NiG and graphene. Generally, metal sample does not show any characteristic peaks in FTIR spectrum.[47] However, the characteristic peak observed at 518 cm^{-1} represents NiO peak (figure 3 (b)). Hence, this confirms the formation of oxide. In the present study, absence of 518 cm^{-1} peak in NiG foam indicates the synthesis of oxide free nickel foam in the presence of graphene.

The Raman spectra of graphene, Ni and NiG are shown in figure 3(c).The spectra of NiG and graphene comprise D and G bands at 1334 and 1598 cm^{-1}, respectively. The D band is attributed to the defects and disorder in the graphitic hexagonal lattice while G band corresponds to E_{2g} mode which is a measure of the vibration of sp^2 bonded carbon atoms in the hexagonal lattice. Raman spectrum of pure Ni foam shows a peak at around 588 cm^{-1} and this peak was ascribed to the oxide layer formed on the Ni surface,[48] while this oxide peak is absent in the NiG foam.

A detailed XPS analysis carried out on Ni and NiG foams are shown in figure 3 (d-g). Figures 3(d) and (f) revealed the presence of Ni $2p_{3/2}$ and $2p_{1/2}$ regions around 856.5 (for NiG) and 870.2 eV (for Ni), respectively. In NiG foam, Ni 2p peak has its twin split spin components with an energy gap around 14 eV where as Ni foam the energy gap was slightly

shifted to 15.54 eV. This can be due to the presence of oxygen functionalities which make the binding energy of Ni shift toward a higher value than that of NiG foam.[49] Figures 3 (e) and (g) show the deconvoluted C1s spectra for NiG and Ni foams, respectively. The high resolution peaks appeared at 284.6 eV corresponding to the presence of C=C sp^2 graphitic carbon in NiG foam, and for Ni foam the peak appeared at 283 eV. The absence of deconvoluted curves in C1s spectra of Ni foam with binding energy lower than 284 eV indicated the absence of graphitic carbon.[27] The area analysis of deconvoluted curves of C1s and Ni2p for NiG foam revealed that 18 % of sp^2 graphitic carbon, 66.3 % of Ni and 15.7 % of oxygen while Ni revealed that 66.3 % of Ni and 33.7% of oxygen.

Due to the ultralow density, hydrophobic nature (due to the presence of surface graphitic layer) and magnetic properties, these NiG foams can be used for selective oil adsorption from water and its tracking using a permanent magnet (see supporting information for further details). It has been previously demonstrated with carbon nanotubes (CNTs) sponges that large quantities of hydrocarbons can be selectively separated using these materials.[50] Since CNTs being expensive, the replacement of CNT sponges with NiG will benefit the applications in these fields. As one of the authors demonstrated with CNT sponges,[50] the adsorbed oils can be burnt and the sponge can also be reused for further oil adsorption and magnetic tracking (supporting information). Moreover, even after burning the adsorbed oil in air, NiG foam did not lose its magnetic properties indicate that the Ni is well protected by a graphene layer.

The impregnation of PMMA into Ni structures resulted into the formation of Ni / PMMA reinforced hybrid porous structures as observed in the FE-SEM image Fig. 4(a). As the PMMA is infiltrated into a pre-shaped Ni sponge, it is observed that the sponge is not squeezing down, while keeping the original shape. The casting at an elevated temperature (50 ^{o}C) leads to formation of reinforced composite solid of Ni / PMMA retaining its original

shape. These composite solids can have potential in various viscoelastic applications (dynamic mechanical analysis results are not shown), whereas, here we demonstrated the synthesis of large area graphene by these composite solids.

Annealing of Ni / PMMA hybrid sponge was carried out under Ar-H_2 atmosphere at 900^{o}C. The motivation behind this experiment was to develop large area interconnected graphene using these 3D scaffolds. Figure 4(b) shows the XRD of the pure crystalline Ni-Graphene hybrid formed from the PMMA after annealing, without the residue of PMMA. The absence of graphitic (004) peak at ~54.7 in the XRD indicates that the formed graphene has no long range order. The formed graphene is separated from Ni scaffold using a water assisted sonication and the graphene is phase separated on the top of the sonicating beaker due to its hydrophobic nature, and the nickel is magnetically separated. The phase separated graphene is scooped out, and can be transferred into any substrates. Figure 4(c) corresponds to the XRD pattern of the graphene separated from annealed Ni / PMMA 3D scaffold. There are no traces of metal / metal oxide impurities in the Raman or XRD. Raman spectrum of the separated graphene is shown in Fig. 4(d). The fluffy, large area interconnected graphene is shown in FE-SEM image, figure 4(e) and an AFM image of the separated graphene shown in figure 4(f) indicates the formation of large area few layered graphene. This indicates that large area interconnected graphene, can be synthesized using these metallic scaffolds as 3D support.

4. Conclusion

A versatile and novel approach has been demonstrated for the synthesis of low density Ni and NiG sponges. This modified polyol method delivers large quantity graphene protected metallic and magnetic nickel sponges, and this study generalises the polyol assisted method for the development of light weight metal sponges where they are protected against the

oxidation by self-assembled thin graphene sheets. Ni / NiG foams act like meso and macro porous 3D scaffolds and it can be mechanically reinforced with other polymers without losing its structural integrity. Later, Ni / PMMA 3D scaffold is demonstrated as template for the synthesis of interconnected large area graphene, and thus developed graphene is separated from the scaffold using a simple water assisted approach.

Acknowledgements

TNN acknowledges DST for financial support in the form of DST-FAST Track scheme (SB/FTP/PS-084/2013: GAP26/13). Financial support through MULTIFUN (CSC 0101) is also highly acknowledged. Authors thank the CSIR-CECRI Central Instrumentation Facility team for helping to handle the analytical instruments and characterisation.

References

1 V. Georgakilas, M. Otyepka, A. B. Bourlinos, V. Chandra, N. Kim, K. C. Kemp, P. Hobza, R. Zboril and K. S. Kim, *Chem. Rev.,* 2012, **112**, 6156-6214.

2 D. Chen, H. Feng and J. Li, *Chem. Rev.,* 2012, **112**, 6027-6053.

3 S. Zhang, Y. Shao, H. G. Liao, J. Liu, I. A. Aksay, G. Yin and Y. Lin, *Chem. Mater.,* 2011, **23**, 1079-1081.

4 Y. Wang, Z. Li, J. Wang, J. Li and Y. Lin, *Trends in Biotechnology,* 2011, **29**, 205-212.

5 D. C. Marcano, D. V. Kosynkin, J. M. Berlin, A. Sinitskii, Z. Sun, A. Slesarev, L. B. Alemany, W. Lu and J. M. Tour, *ACS Nano,* 2010, **4**, 4806-4814.

6 Y. Zhu , S. Murali , W. Cai , X. Li , J. W. Suk , J. R. Potts and R. S. Ruoff, *Adv. Mater.,* 2010, **22**, 3906-3924.

7 D. A. Dikin, S. Stankovich, E. J. Zimney, R. D. Piner, G. H. B. Dommett, G. Evmenenko, S. B. T. Nguyen and R. S. Ruoff, *Nature,* 2007, **448**, 457-460.

8 L. Jiao, X. Wang, G. Diankov, H. Wang and H. Dai, *Nat. Nanotechnol.,* 2010, **5**, 321-325.

9 D. V. Kosynkin, A. L. Higginbotham, A. Sinitskii, J. R. Lomeda, A. Dimiev, B. K. Price and J. M.Tour,*Nature,*2009, **458**, 872-876.

10 X. Yang, X. Dou, A. Rouhanipour, L. Zhi, H. J. Rader and K. Mullen, *J. Am. Chem. Soc.,* 2008, **130**, 4216-4217.

11 D. Wei, Y. Liu, H. Zhang, L. Huang, B. Wu , J. Chen and G. Yu, *J. Am. Chem. Soc.,* 2009, **131**, 11147-11154.

12 M. Terrones, A. R. B. Méndez, J. C. Delgado, F. L. Urías, Y. I. V. Cantú, F. J. R. Macías, A. L. Elias, E. M. Sandoval, A. G. C. Marquez, J. C. Charlier and H. Terrones, *Nanotoday,* 2010, **5**, 351-372.

13 Z. H. Sheng, L. Shao, J. J. Chen, W. J. Bao, F. B. Wang and X. H. Xia, *ACS Nano,* 2011, **5**, 4350-4358.

14 T. N. Narayanan, Z. Liu, P. R. Lakshmy, W. Gao , Y. Nagaoka ,D. Sakthi Kumar, J. Lou, R. Vajtai and P. M. Ajayan, *Carbon,* 2012, **50**, 1338-1345.

15 Y. Zheng, Y. Jiao, L. Ge, M. Jaroniec and S. Z.Qiao, *Angew.Chem.Int. Ed,.* 2013, **125**, 3192-3198.

16 H. P. Cong, X. C. Ren, P. Wang and S. H. Yu, *ACS Nano,* 2012, **6**, 2693-2703.

17 M. A. Worsley, P. J. Pauzauskie, T. Y.Olson, J. Biener, J. H. Satcher, Jr and T. F. Baumann, *J. Am. Chem. Soc.,* 2010, **132**, 14067-14069.

18 Z. Sui, Q. Meng, X. Zhang, R. Mab and B. Caob, *J. Mater. Chem.,* 2012, **22**, 8767-8771.

19 H. Bai, C. Li, X. Wang and G. Shi, *J. Phys. Chem. C.,* 2011, **115**, 5545-5551.

20 Z. Zhao, X. Wang, J. Qiu, J. Lin and D. Xu, *Rev. Adv. Mater.Sci.,* 2014, **36**, 137-151.

21 Y. Xu , Z. Lin , X. Huang , Y. Wang ,Y. Huang and X. Duan, *Adv. Mater*., 2013, **25**, 5779-5784.

22 M. Park, B. Pant, J. Choi, Y. W. Park, C. Lee, H. K. Shin, S .J. Park and H. Y. Kim, *Carbon,* 2014, **15**, 136-141.

23 J. Kuang, L. Liu, Y. Gao, D. Zhou, Z. Chen, B. Hana and Z. Zhang, *Nanoscale,* 2013, **5**, 12171-12177.

24 X. Huang, B. Sun, D. Su, D. Zhao and G. Wang, *J. Mater. Chem.A,* 2014, **2**, 7973-7979.

25 X. Dong, Y. Ma, G. Zhu, Y. Huang, J. Wang, M. B. C. Park, L. Wang, W. Huang and P. Chen, *J. Mater. Chem.,* 2012, **22**, 17044-17048.

26 Y. Xue, J. Liu, H. Chen, R. Wang, D. Li, J. Qu and L. Dai, *Angew. Chem. Int. Ed.,* 2012, **51**, 1-5.

27 Z. Chen, W. Ren, L. Gao, B. Liu, S. Pei and H. M. Cheng, *Nat. Mater.,* 2011, **10**, 424-428.

28 M. G. Hahm, A. L. M. Reddy, D. P. Cole, M. Rivera, J. A.Vento, J. Nam, H. Y. Jung, Y. L. Kim, N. T. Narayanan, D. P. Hashim, C. Galande, Y. J. Jung, M. Bundy, S. Karna, P. M. Ajayan and R. Vajtai, *Nano Lett*., 2012, **12**, 5616-5621.

29 P. M .Sudeep, T. N. Narayanan, A. Ganesan, M. M. Shaijumon, H. Yang, S. Ozden, P. K. Patra, M. Pasquali, R. Vajtai, S. Ganguli, A. K. Roy, M. R. Anantharamanand P. M .Ajayan, *ACS Nano,* 2013, **7**, 7034-7040.

30 Y. Xu, Q. Wu, Y. Sun, H. Bai and G. Shi, *ACS Nano,* 2010, **4**, 7358-7362.

31 W. Chen, Z. Fan, G. Zeng and Z. Lai, *J. Power Sources,* 2013, **225**, 251-256.

32 P. Trinsoutrot, H. Vergnes and B. Caussat, *Mater. Sci. Eng. B,* 2014, **179**, 12-16.

33 B. Tang, G. Hu, H. Gao and Z. Shi, *J. Power Sources,* 2013, **234**, 60-68.

34 F. Ravani, K. Papagelis, V. Dracopoulos, J. Parthenios, K. G. Dassios , A. Siokou and C. Galiotis, *Thin Solid Films,* 2013, **527**, 31-37.

35 H. Bi, F. Huanga, Y. Tang, Z. Liu, T. Lin, J. Chen and W. Zhao, *Electrochimica Acta,* 2013, **88**, 414-420.

36 B. Sun, X. Huang, S. Chen, P. Munroe and G. Wang, *Nano lett.,* 2014, **14(6)**, 3145-3152.

37 H. Huang, Y. Tang, L. Xu, S. Tang and Y. Du, *Appl. Mater. Interfaces,* 2014, DOI-org/10.1021/am501635h.

38 X. Cao, Y. Shi, W. Shi, G. Lu, X. Huang, Q. Yan, Q. Zhang and H. Zhang, *Small,* 2011, **22**, 3163-3268.

39 X. Dong, Y. Cao, J. Wang, M. B. C. Park, L. Wang, W. Huang and P. Chen, *RSC Adv.,* 2012, **2**, 4364-4369.

40 Z. Chen, W. Ren, L. Gao, B. Liu, S. Pei and H. M. Cheng, *Nat. Mater*. 2011, **10**, 424-428.

41 H. Wang, H. S. Casalongue, Y. Liang and H. Dai, *J. Am. Chem. Soc.,* 2010, **132**, 7472-7477.

42 A. N. Golikand, M. Asgari, M. G. Maragheh and S. Shahrokhian, *J. Electroanal. Chem.,* 2006, **588,** 155-160.

43 L. Yang, L. Qian, X. Tian, J. Li, J. Dai, Y. Guo and D. Xiao, *Chem. Asian J.* ,2014, **9**, 1579-1585.

44 Y. Zhu, L. Li, C. Zhang, G. Casillas, Z. Sun, Z. Yan, G. Ruan, Z. Peng, A. Rahman, O. Raji, C. Kittrell, R. H. Hauge and J. M. Tour, *Nature Commun.,* 2012, **3 (1225)**, 1-7.

45 A. P. Reena Mary, C. S. SuchandSandeep, T. N. Narayanan, R. Philip, P. Moloney, P. M. Ajayan and M. R. Anantharaman, *Nanotechnology,* 2011, **22**, 1-7.

46 J. Zhang, H. Yang, G. Shen, P. Cheng, J. Zhangand S. Guo, *Chem. Comm*.,2010,**46**, 1112-1114.

47 D. Senthamilselvan, A. Chezhian, N. Kabilan, T. S. Kumar and N. S. Kumaran, *Int. J. Environ. Sci.,* 2012, **2**, 1976-1983.

48 C. Luo, D. Li, W. Wu, Y. Zhang and C. Pan, *RSC Adv.,* 2014, **4**, 3090-3095.

49 K. S. Kim and N. Winograd, *Surf. Sci.,* 1974, **43**, 625-643.

50 D. P. Hashim, N. T. Narayanan, J. M. R. Herrera, D. A. Cullen, M. G. Hahm, P. Lezzi, J. R. Suttle, D. Kelkhoff, E. M. Sandoval, S. Ganguli, A. K. Roy, D. J. Smith, R. Vajtai, B. G. Sumpter, V. Meunier, H. Terrones, M. Terrones and P. M.Ajayan, *Sci. Rep.,* 2012, **2(363)**, 1-8.

Figure Captions

Figure 1: Schematic of the synthesis of low density, magnetic, Ni and NiG foams. Their light weight, porous and magnetic natures are demonstrated.

Figure 2: FE-SEM images of (a) Ni and (b) NiG foams under different magnification with the inset showing the same at a higher magnification. (c) and (d) show the EDS profiles across Ni and NiG foams.TEM images of (e) Ni and (f) NiG foams under different magnifications, while inset shows their corresponding SAED pattern of the respective regions.

Figure 3: (a) XRD patterns (b) FTIR spectra and (c) Laser Raman spectra plotted for Ni, NiG foams and graphene. (d), (e), (f), and (g) correspond to the deconvoluted Ni_{2p} and C_{1s} XPS spectra of Ni (d & e) and NiG (f & g) foams.

Figure 4: (a) FE-SEM microstructure of porous NiG / PMMA (b) XRD patterns of annealed Ni/PMMA (top) and (c) after separating Ni (bottom), (d) Raman spectrum of Ni / PMMA derived graphene (e) FE-SEM and (f) AFM image of large area Ni / PMMA derived graphene.

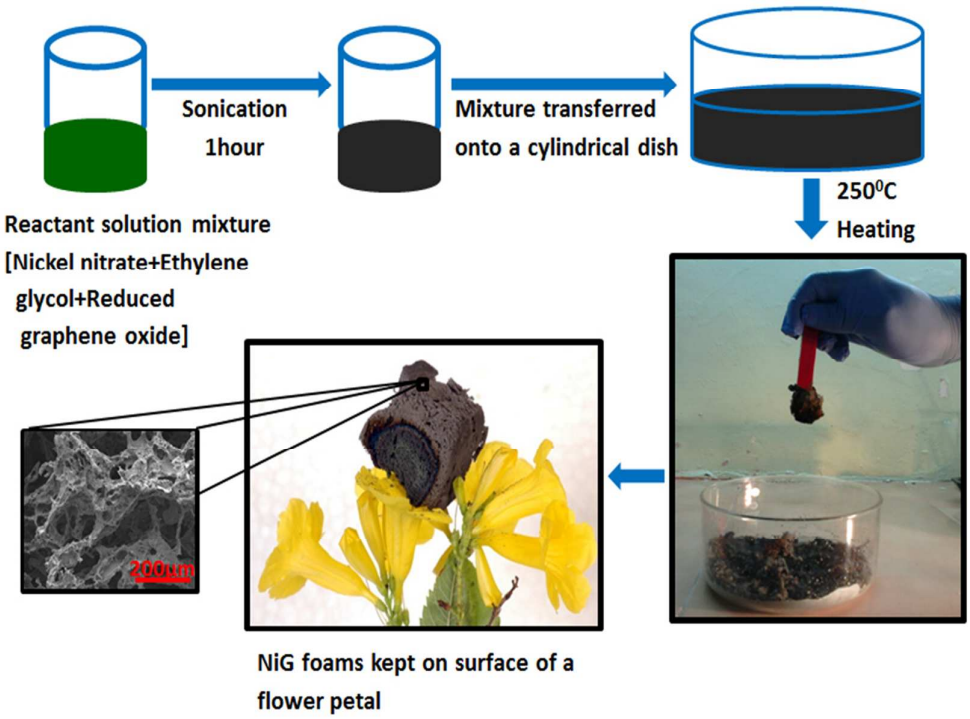

Fig 1:

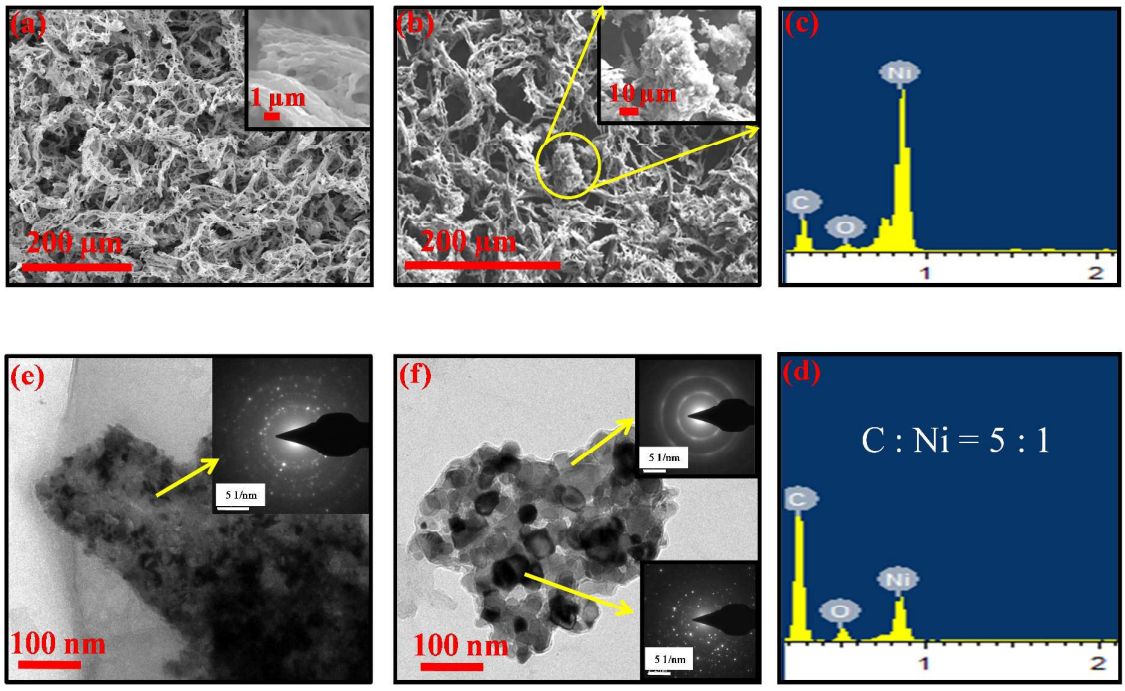

Fig. 2:

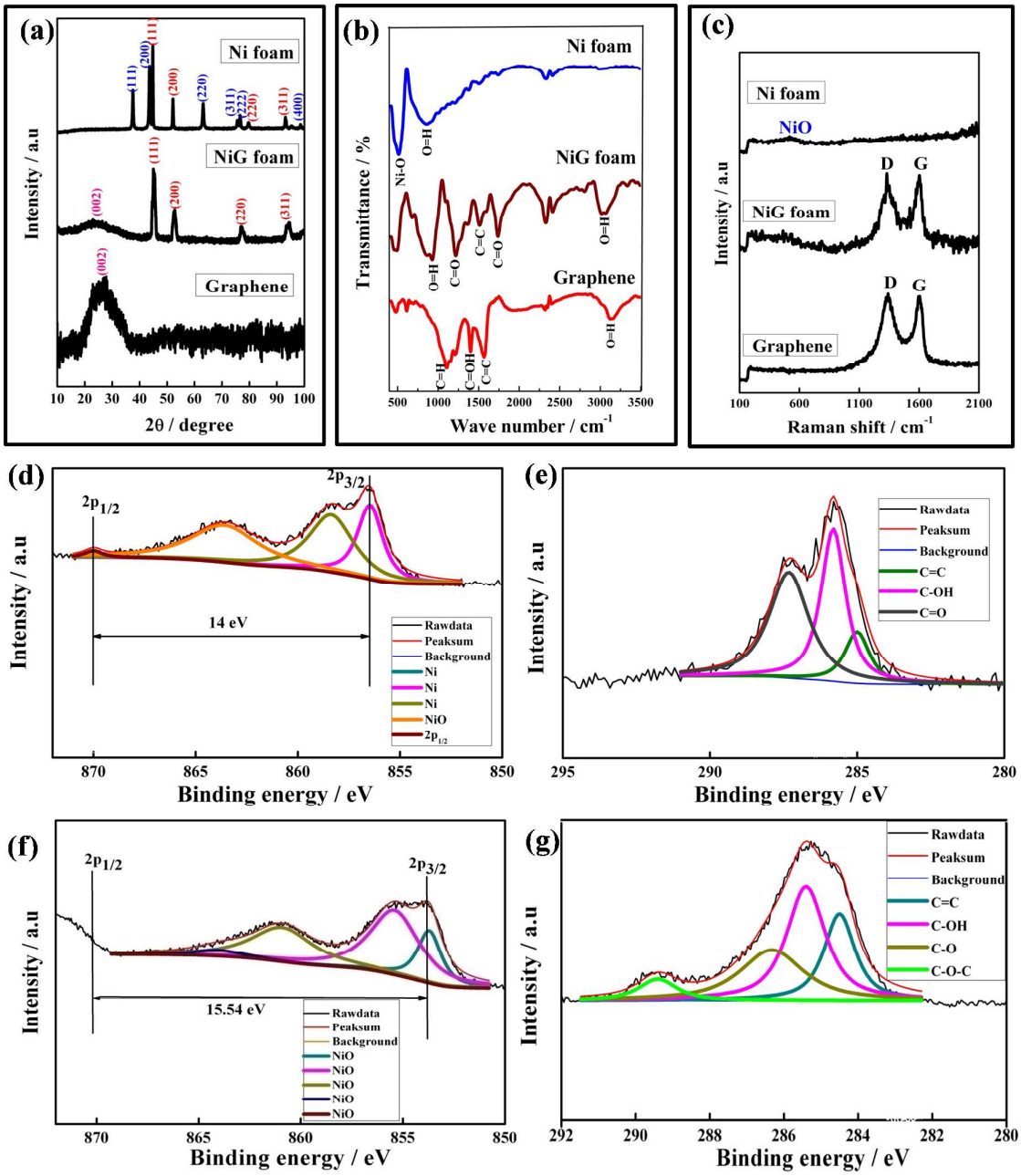

Fig. 3:

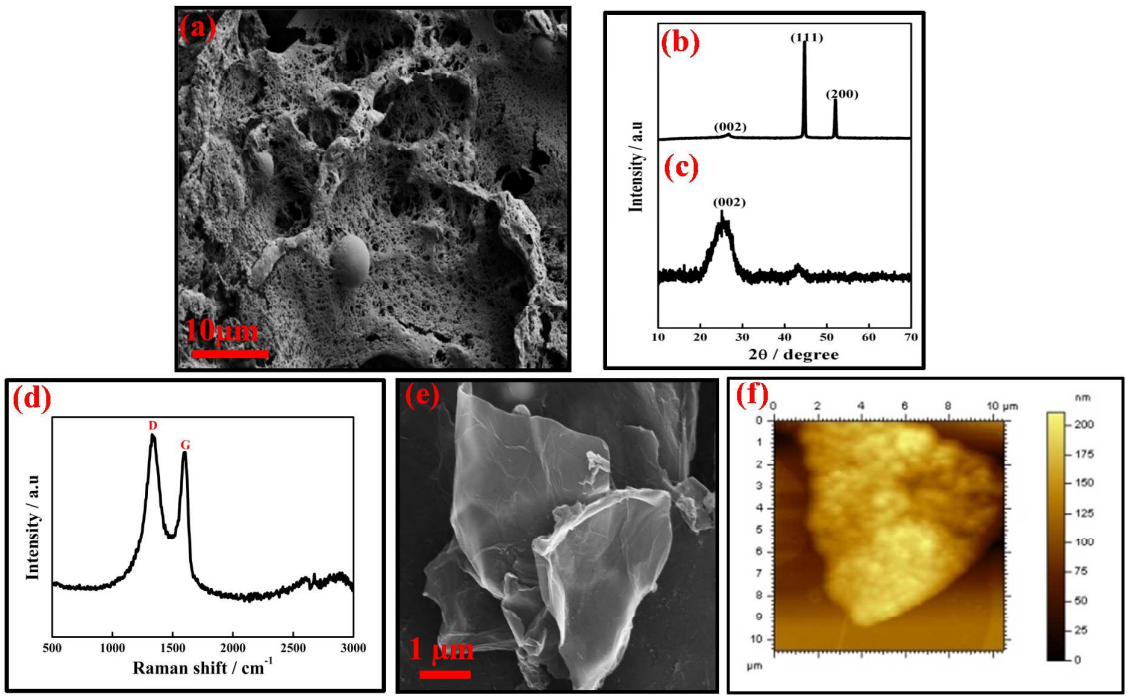

Fig. 4:

Supporting Information

Self-Protected Nickel-Graphene Hybrid Low Density 3D Scaffolds

Moab Rajan Philip[a], T. N. Narayanan[b,*], M. Praveen Kumar[b], Shashi BhushanArya[a] and Deepak K. Pattanayak[b,*]

[a]National Institute of Technology, Surathkal, Karnataka, India.

[b]CSIR-Central Electrochemical Research Institute, Karaikudi, Tamilnadu, India.

(Corresponding Authors:tn_narayanan@yahoo.com(T. N. N.),pattanayak1977@gmail.com (D.K.P.))

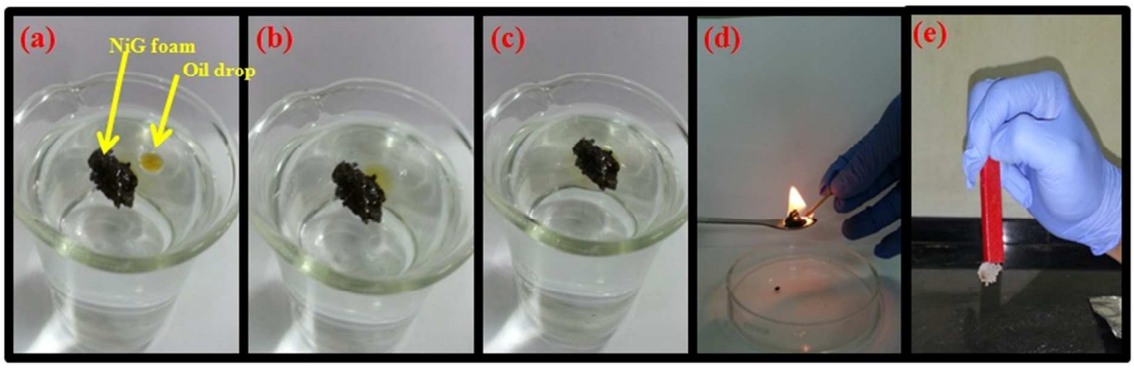

Figure S1: (a), (b), and (c) Figures depicting the adsorption of oil on the surface of NiG foam including the migration of oil (d) the presence of oil inside NiG is verified by burning the foam in air making it reusable as well as retaining magnetic nature (e) depicting that NiG foam where Ni foam surrounded by graphene does not oxidise upon burning in air and still the magnetic nature is retrieved.